A method for generating fully non-stationary and spectrum-compatible ground motion vector processes

By

Pierfrancesco Cacciola* and George Deodatis**

* *School of Environment and Technology, University of Brighton, Lewes road, BN24GJ, Brighton, UK*

** *Department of Civil Engineering and Engineering Mechanics, Columbia University, New York, NY 10027*

ABSTRACT:

Earthquake ground motion spatial variability can influence significantly the response of certain structures. In order to accurately evaluate probabilistic characteristics of the seismic response of structures, the Monte Carlo simulation technique is still the only universal method of analysis when strong nonlinearities and input uncertainties are involved. Consequently, realizations of ground motion time histories taking into account both time and spatial variability need to be generated. Furthermore, for some design applications, the generated time histories must also satisfy the provision imposed by certain seismic codes stating that they have to be also response-spectrum-compatible. For these purposes, a spectral-representation-based methodology for generating fully non-stationary and spectrum-compatible ground motion vector processes at a number of locations on the ground surface is proposed in this paper. The simulated time histories do not require any iterations on the individual generated sample functions so that Gaussianity and prescribed coherence are suitably preserved. The methodology has also the advantage of providing the fully non-stationary and spectrum-compatible cross-spectral density matrix of the ground motion time-histories that can be used for reliability studies in an analytic stochastic fashion.

Keywords: Ground motion simulation, vector process, non-stationarity, time-variability, spatial variability, spectrum-compatible, code provisions.

1 INTRODUCTION

Ground motion arising from seismic waves is a phenomenon that by its nature varies with time and in space. Commonly, in earthquake engineering practice, the attention is focused on the time variability component and its effects on the structural response. On the other hand, it is well known that the spatial variability of earthquake ground motion can influence significantly the response of structures, especially if they are long and/or rigid. In this context, a number of contributions has been devoted to the study of the effects of spatial variability on various structures including buildings [1-4], bridges [5-8], arcs [9,10], dams [11], rigid foundations [12,13], pipelines [14,15], transmission lines [16], and nuclear power plants [17]. Readers could also refer to the monograph by Zerva [18] for an overview of the engineering applications in which ground motion spatial variability has been taken into account. The phenomenon of ground motion spatial variability is affected by several factors, i.e. source patterns, path, site effects, etc., that generally cannot be described in a deterministic fashion. Consequently, only a probabilistic approach can provide a rigorous representation of the spatial variability of earthquake ground motion. As a consequence, the computation of structural response is a challenging task for which both ground motion time and spatial variability have to be taken into account. Different strategies have been proposed in the last 2-3 decades for predicting the pertinent structural response. Response spectrum based techniques [19-21] are certainly the simplest ones. These methods are very attractive for design purposes due to their simplicity, but can become inaccurate, especially in the case of nonlinearly behaving structures. Analytical approaches [22,23] based on random vibration theory have captured the attention of researchers and practitioners due to their rigorous mathematical basis and their efficiency in the case of linear/linearized structures. However, such analytical approaches are not

commonly used in practice and possess the limitation to be difficult to apply in the presence of strong nonlinearities. To date, Monte Carlo simulation techniques still remain the only universal method of analysis when strong nonlinearities as well as input uncertainties are involved. In this regard, the accurate simulation of ground motion time histories is the first step in the analysis of the effects of both time and spatial variability of earthquake ground motion. To accomplish this objective, various simulation techniques have been proposed for generating ground motion time histories taking into account spatial variability [24-36]. Readers could refer to the monograph by Zerva [18] for an in-depth discussion of the state of the art along with the challenges involved in modelling the spatial variability of earthquake ground motion. Spectral-representation-based simulation techniques [27,28,37,38] are among the most widely-used today for this purpose. Accordingly, earthquake ground motion is modelled as a Gaussian, non-stationary, multi-variate vector process, fully defined by its evolutionary cross-spectral density matrix. Spatial variability can be described by the off-diagonal elements of this matrix through coherence functions and apparent velocity of wave propagation.

Interestingly, various international seismic codes allow the use of simulated ground motion time-histories for the seismic design of structures. For this purpose, the simulated time-histories have to be spectrum-compatible, i.e. the average response spectrum computed using simulated time histories has to match the target response spectrum provided by the code over a fixed frequency range and with a code-specified tolerance. This means that the simulated ground motion time histories have to be non-stationary in time, spatially variable in space, and spectrum-compatible. The number of contributions devoted to the simulation of spectrum-compatible, uni-variate, ground motions time histories is significant. However, relatively few contributions have considered the case of multi-variate (vector) processes accounting for spatial variability. Hao et al. [39] proposed a method that adjusts independently simulated quasi-stationary time histories in order to make them compatible with the prescribed response spectrum. This adjustment is performed by Fourier transforming each time history to the frequency domain, multiplying its frequency domain Fourier

transform by the ratio of the prescribed response spectrum over the computed response spectrum of the non-stationary time history, and then inverse transforming the product back to the time domain. Deodatis [38] proposed a methodology for generating quasi-stationary spectrum-compatible ground motion vector processes starting from the generation of ergodic, stationary time histories that are compatible with a coherence function and a velocity of wave propagation but not with the prescribed response spectrum. After modulating the generated time histories, the matching of the response spectra is achieved by the successive upgrading of the power spectral density functions of the components of the vector process.

It is well known that the dynamic response of nonlinear structures is highly influenced by the non-stationary behaviour of the input [40-42]. Consequently, for a more reliable representation of the seismic structural response, both the amplitude and frequency variation of ground motion time histories have to be accounted for. This can be achieved using the concept of evolutionary power spectra [43]. According to evolutionary power spectrum theory, in such a case involving so-called amplitude and frequency modulation, the elements of the cross-spectral density matrix have to be non-separable functions of both frequency and time. Recently, Sarkar and Gupta [44] proposed an iterative methodology for generating fully non-stationary spectrum-compatible vector processes using a wavelet-based approach (it should be noted that “fully non-stationary” stands for a non-stationary process with amplitude and frequency variation in time, while “quasi-stationary” stands for a non-stationary process with only amplitude variation in time). The method assumes that a suitable accelerogram conforming to the local source and site condition is available. Furthermore, the accelerogram is modified so as to be spectrum-compatible to a design response spectrum, assumed the same for each free-field location.

In this paper, a novel methodology for generating fully non-stationary, spectrum-compatible, ground motion vector processes is proposed. The methodology considers that the ground motion vector process is modelled as the superposition of two contributions: the first one is a known fully non-stationary component modelled as a non-separable *m*-variate non-stationary stochastic process

representative of local geological and seismological conditions. The second one is a corrective term modeled by an *m*-variate quasi-stationary non-stationary process. The cross-spectral density matrix of the corrective term is determined extending the procedure proposed by Cacciola [45] for scalar processes to the case of vector processes. After determining the evolutionary cross-spectral density matrix of the vector process resulting from the aforementioned superposition, ground motion sample functions at different locations compatible with prescribed response spectra and preserving a given coherence function are generated using the procedure proposed by Deodatis [38]. It has to be emphasized that the simulated time histories do not require any iterations for matching the prescribed response spectra.

2 *m*-VARIATE NON-STATIONARY STOCHASTIC GROUND MOTION PROCESSES

Following the spectral-representation methodology (e.g. Shinozuka and Deodatis [27]), consider the 1D-*m*V (one-dimensional, *m*-variate) non-stationary ground motion stochastic vector process, whose components $f_j^0(t)$, $(j=1,...,m)$ have zero mean:

$$E\left[f_j^0(t)\right] = 0, \qquad (j=1,...,m) \tag{1}$$

cross-correlation matrix given by:

$$\mathbf{R}_f^0(t,t+\tau) = \begin{bmatrix} R_{11}^0(t,t+\tau) & R_{12}^0(t,t+\tau) & \cdots & R_{1m}^0(t,t+\tau) \\ R_{21}^0(t,t+\tau) & R_{22}^0(t,t+\tau) & \cdots & R_{2m}^0(t,t+\tau) \\ \vdots & \vdots & \ddots & \vdots \\ R_{m1}^0(t,t+\tau) & R_{m2}^0(t,t+\tau) & \cdots & R_{mm}^0(t,t+\tau) \end{bmatrix}, \tag{2}$$

and corresponding cross-spectral density matrix with evolutionary power spectrum given by [43]:

$$\mathbf{S}_f^0(\omega,t)=\begin{bmatrix} S_{11}^0(\omega,t) & S_{12}^0(\omega,t) & \cdots & S_{1m}^0(\omega,t) \\ S_{21}^0(\omega,t) & S_{22}^0(\omega,t) & \cdots & S_{2m}^0(\omega,t) \\ \vdots & \vdots & \ddots & \vdots \\ S_{m1}^0(\omega,t) & S_{m2}^0(\omega,t) & \cdots & S_{mm}^0(\omega,t) \end{bmatrix} \tag{3}$$

Due to the non-stationarity of the vector process, the cross-correlation matrix is a function of both time t and time lag τ, while the cross-spectral density matrix is a function of both frequency ω and time t. It has to be emphasized that under the hypothesis of fully non-stationary processes (non-stationary processes with amplitude and frequency modulation), the cross-spectral density matrix is a non-separable function of frequency ω and time t. Specifically for the case of earthquake ground motion, the elements of the cross-spectral density matrix with evolutionary power can be expressed in the following special form:

$$\begin{aligned} &S_{jj}^0(\omega,t)=\left|A_j(\omega,t)\right|^2 S_j(\omega), && j=1,2,...,m \\ &S_{jk}^0(\omega,t)=A_j(\omega,t)A_k(\omega,t)\sqrt{S_j(\omega)S_k(\omega)}\Gamma_{jk}(\omega), && j,k=1,2,...,m;\quad j\neq k \end{aligned} \tag{4}$$

where $A_j(\omega,t)$ and $S_j(\omega)$ $(j=1,2,...,m)$ are the (non-separable) modulating function and the (stationary) power spectral density function of component $f_j^0(t)$, $(j=1,2,...,m)$, respectively, and $\Gamma_{jk}(\omega)$, $(j,k=1,2,...,m;\ j\neq k)$ is the complex coherence function between $f_j^0(t)$ and $f_k^0(t)$. The cross spectral density matrix $\mathbf{S}_f^0(\omega,t)$ is Hermitian and satisfies the following properties (e.g. Deodatis [38]):

$$S_{jj}^0(\omega,t)=S_{jj}^0(-\omega,t), \qquad j=1,2,...,m \quad \forall t \tag{5}$$

with the off-diagonal elements being generally complex functions of ω satisfying:

$$S_{jk}^0(\omega,t)=S_{jk}^{0*}(-\omega,t), \qquad j,k=1,2,...,m;\ j\neq k;\quad \forall t \tag{6}$$

and

$$S_{jk}^0(\omega,t)=S_{kj}^{0*}(\omega,t), \qquad j,k=1,2,...,m;\ j\neq k;\quad \forall t \tag{7}$$

where the asterisk denotes the complex conjugate. Moreover, the elements of the cross-correlation matrix are related to the corresponding elements of the cross-spectral density matrix through the following transformations:

$$R_{jj}^{0}(t,t+\tau)=\int_{-\infty}^{\infty}A_j(\omega,t)A_j(\omega,t+\tau)S_j(\omega)e^{i\omega\tau}d\omega;\quad j=1,2,...,m \tag{8}$$

$$R_{jk}^{0}(t,t+\tau)=\int_{-\infty}^{\infty}A_j(\omega,t)A_k(\omega,t+\tau)\sqrt{S_j(\omega)S_k(\omega)}\Gamma_{jk}(\omega)e^{i\omega\tau}d\omega;\quad j,k=1,2,...,m;\ \ j\neq k \tag{9}$$

For the special case of uniformly modulated nonstationary stochastic vector process, the modulating functions $A_j(\omega,t)$ $(j=1,2,...,m)$ are independent of the frequency ω, that is:

$$A_j(\omega,t)=A_j(t),\qquad j=1,2,...,m \tag{10}$$

In this special case, equations (8) and (9) reduce to:

$$R_{jj}^{0}(t,t+\tau)=A_j(t)A_j(t+\tau)\int_{-\infty}^{\infty}S_j(\omega)e^{i\omega\tau}d\omega;\quad j=1,2,...,m \tag{11}$$

$$R_{jk}^{0}(t,t+\tau)=A_j(t)A_k(t+\tau)\int_{-\infty}^{\infty}\sqrt{S_j(\omega)S_k(\omega)}\Gamma_{jk}(\omega)e^{i\omega\tau}d\omega;\quad j,k=1,2,...,m;\ \ j\neq k \tag{12}$$

3. SIMULATION FORMULA FOR *m*-VARIATE NON-STATIONARY STOCHASTIC PROCESSES

According to the algorithm in [38], in order to simulate the 1D-*m*V non-stationary ground motion vector process, $\boldsymbol{f}^{0}(t)$, the evolutionary cross-spectral density matrix $\mathbf{S}_f^{0}(\omega,t)$ is first decomposed at every time instant t using Cholesky's method into the following product:

$$\mathbf{S}_f^{0}(\omega,t)=\mathbf{H}(\omega,t)\mathbf{H}^{T*}(\omega,t) \tag{13}$$

where $\mathbf{H}(\omega,t)$ is a lower triangular matrix and the superscript T denotes the transpose of a matrix. $\mathbf{H}(\omega,t)$ is written as:

$$\mathbf{H}(\omega,t)=\begin{bmatrix} H_{11}(\omega,t) & 0 & \cdots & 0 \\ H_{21}(\omega,t) & H_{22}(\omega,t) & \cdots & 0 \\ \vdots & \vdots & \ddots & \vdots \\ H_{m1}(\omega,t) & H_{m2}(\omega,t) & \cdots & H_{mm}(\omega,t) \end{bmatrix}. \tag{14}$$

The diagonal elements of $\mathbf{H}(\omega,t)$ are real and non-negative functions of ω satisfying:

$$H_{jj}(\omega,t)=H_{jj}(-\omega,t), \qquad j=1,2,...,m; \quad \forall t \tag{15}$$

while the off-diagonal elements are generally complex functions of ω. Once the cross-spectral density matrix $\mathbf{S}_f^0(\omega,t)$ is decomposed according to equations (13) and (14), the non-stationary ground motion vector process $f_j^0(t), \quad j=1,2,...,m$ can be simulated by the following series as $N\to\infty$

$$f_j(t)=2\sum_{r=1}^{m}\sum_{s=1}^{N}\left|H_{jr}(\omega_s,t)\right|\sqrt{\Delta\omega}\cos\left[\omega_s t-\vartheta_{jr}(\omega_s,t)+\phi_{rs}\right], \quad j=1,2,...,m \tag{16}$$

where:

$$\vartheta_{jk}(\omega,t)=\tan^{-1}\left(\frac{\mathrm{Im}\left[H_{jk}(\omega,t)\right]}{\mathrm{Re}\left[H_{jk}(\omega,t)\right]}\right) \tag{17}$$

with $\mathrm{Im}[\bullet]$ and $\mathrm{Re}[\bullet]$ denoting the imaginary and real part of a complex number, respectively. Note that in eq. (16), superscript "0" is omitted to distinguish the vector process $\boldsymbol{f}^0(t)$ from its simulation $\boldsymbol{f}(t)$. The discretization in the frequency domain is done as follows:

$$\omega_s=s\,\Delta\omega, \qquad s=1,2,...,N; \qquad \Delta\omega=\frac{\omega_c}{N} \tag{18}$$

In equation (18), ω_c represents an upper cut-off frequency beyond which the elements of the cross-spectral density matrix may be assumed to be zero at any time instant t. Furthermore, the $\phi_{rs}\,(r=1,2,...,m;\ s=1,2,...,N)$ are m sequences of N independent random phase angles distributed uniformly over the interval $[0,2\pi]$.

4. PROPOSED APPROACH FOR GENERATING FULLY NON-STATIONARY SPECTRUM-COMPATIBLE GROUND MOTION VECTOR PROCESSES

The elastic response spectrum approach is the most commonly used method to design structures against seismic action according to various international codes. Alternatively, "appropriate simulated" ground motion time-histories can be used for seismic design applications [46], [47]. For this purpose, the simulated time-histories have to be spectrum-compatible, i.e. the average response spectrum computed using simulated time histories has to match the target response spectrum provided by the code over a fixed frequency range and with a code-specified tolerance. That is:

$$\left|\frac{RSA^{(j)}(\omega)-RSA^{(f_j)}(\omega)}{RSA^{(j)}(\omega)}\right|\le\varepsilon\ ,\qquad \forall\ \omega_l\le\omega\le\omega_u\qquad (j=1,...,m) \tag{19}$$

where $RSA^{(j)}(\omega)$ is the *j*-th target response spectrum, $RSA^{(f_j)}(\omega)$ is the *j*-th ensemble-averaged response spectrum of the simulated ground motion vector process $f_j(t),\quad j=1,2,...,m$ and ε is a code-specified tolerance, commonly defined as a constant value (and not a function of frequency). Note that seismic codes impose only the value of the tolerance ε and of the bounds ω_l and ω_u. No specific methodology is suggested to simulate the spectrum-compatible accelerograms (see e.g. [46,47]).

A spectral representation based approach will be used here for generating fully non-stationary spectrum-compatible ground motion vector processes. It should be mentioned that simulated ground motion time-histories are generally criticized for failing to rigorously describe the physical characteristics of strong ground motion. This is due to the fact that the non-stationary waveforms of the actual seismic time histories are strongly influenced by several factors (such as the seismic source rupture pattern, inhomogeneities in the soil mass, etc.) that are not fully accounted for in the simulation process. To overcome this drawback, the non-stationary as well as the spatial variability features of simulated ground motion should be selected so as to reflect local geological and seismological conditions. This can be achieved by using recorded local accelerograms. The problem

is that recorded accelerograms are not in general spectrum-compatible. To address this problem, the main idea of this work is that the non-stationary spectrum-compatible ground motion vector process is given by the superposition of two contributions: the first one is a fully non-stationary vector process $f_j^L(t),\ (j=1,...,m)$ with known non-separable cross-spectral density matrix representative of geological and seismological conditions at the site; while the second one is a quasi-stationary vector process $f_j^C(t),\ (j=1,...,m)$ with unknown cross-spectral density matrix, whose objective is to correct each component of $f_j^L(t),\ (j=1,...,m)$ in order to make them spectrum-compatible. That is:

$$f_j^{SC}(t) = f_j^L(t) + f_j^C(t), \qquad (j=1,2,...,m) \tag{20}$$

where superscript “L” stands for “local” (to emphasize that the first term reflects non-stationarity and spatial variability pertinent to the site where the ground motion is modelled); superscript “C” stands for “corrective” (to emphasize that the second term is devoted to adjust the process $f_j^L(t),\ (j=1,...,m)$ to make it spectrum-compatible), and the superscript “SC” stands for “spectrum-compatible” . The non-stationary characteristics of the simulated ground motion vector process – as well as of its spatial variability – are taken into account through a pertinent representation of vector process $f_j^L(t),\ (j=1,...,m)$ that can be pursued using various approaches (see e.g. [38], [40]). The spectrum-compatible condition imposed by the seismic code is satisfied through an appropriate definition of the corrective process $f_j^C(t),\ (j=1,...,m)$ that has to be determined so as to preserve the main features of vector process $f_j^L(t),\ (j=1,...,m)$.

Accordingly, it is assumed that $f_j^C(t),\ (j=1,...,m)$ is a quasi-stationary process with evolutionary power spectral density for each individual component given by:

$$S_j^C(\omega,t) = \varphi_j^2(t) S_j^C(\omega), \qquad (j=1,2,...,m) \tag{21}$$

where $\varphi_j(t)$ is the j-th modulating function determined so as to preserve the amplitude time variability of process $f_j^L(t)$ [45], while $S_j^C(\omega)$ is the *j*-th (stationary) power spectral density of the corrective process that needs to be determined.

Taking into account now eq. (20), the response spectra $RSA^{(f_j^{SC})}(\omega)$, $(j=1,...,m)$ can be approximately determined, in analogy with the "square root of sum of squares" (SRSS) modal combination rule proposed by Rosenblueth [48], by the following equation:

$$RSA^{(f_j^{SC})}(\omega)=\sqrt{\left[RSA^{(f_j^{L})}(\omega)\right]^2+\left[RSA^{(f_j^{C})}(\omega)\right]^2} \quad , \ (j=1,2,...,m) \tag{22}$$

In eq (22) $RSA^{(f_j^{L})}(\omega)$ and $RSA^{(f_j^{C})}(\omega)$ are the response spectra of the j-th component of processes $f_j^L(t)$ and $f_j^C(t)$, $(j=1,...,m)$, respectively. Considering that eq. (20) involves stochastic processes, eq. (22) should be interpreted here in an ensemble average sense. This means that it is an ensemble-averaged $RSA^{(f_j^{SC})}(\omega)$ that is supposed to match the target response spectra $RSA^{(j)}(\omega)$; $j=1,2,...,m$ prescribed by the seismic code.

The basic idea of the paper can now be summarized as follows: $RSA^{(f_j^{C})}(\omega)$ in eq. (22) can be computed as $RSA^{(f_j^{SC})}(\omega)$ and $RSA^{(f_j^{L})}(\omega)$ are known ($RSA^{(f_j^{SC})}(\omega)$ is supposed to be equal to $RSA^{(j)}(\omega)$ and $RSA^{(f_j^{L})}(\omega)$ can be estimated as $f_j^L(t)$ is known). The probabilistic characteristics of $f_j^C(t)$ can be computed from $RSA^{(f_j^{C})}(\omega)$; $j=1,2,...,m$. The aforementioned basic idea is described in some detail in the following. The response spectrum $RSA^{(f_j^{C})}(\omega)$ can be approximately determined through the following first crossing problem [49]:

$$RSA^{(f_j^{C})}(\omega_0)=\omega_0^2\eta_{U^C}^{(j)}(\omega_0,\zeta_0,\lambda_{0,U^C}^{(j)}(\omega_0),\lambda_{1,U^C}^{(j)}(\omega_0),\lambda_{2,U^C}^{(j)}(\omega_0),T_s,p=0.5)\sqrt{\lambda_{0,U^C}^{(j)}(\omega_0)} \tag{23}$$

where $\eta_{U^C}^{(j)}$ is the peak factor, ζ_0 is the damping ratio, T_s is the duration of the observing window set equal to the strong motion phase of the process $f_j^L(t)$, p is the non-exceedance probability, and $\lambda_{i,U^C}^{(j)}$ $(i=0,1,2)$ are the response spectral moments defined as:

$$\lambda_{i,U^C}^{(j)}(\omega_0) = \int_0^\infty \omega^i \left|H(\omega_0,\omega)\right|^2 G_j^C(\omega) d\omega \tag{24}$$

where $\left|H(\omega_0,\omega)\right|^2 = \left((\omega_0^2-\omega^2)^2 + 4\zeta_0^2\omega_0^2\omega^2\right)^{-1}$ is the energy transfer function and $G_j^C(\omega)$ $(=2S_j^C(\omega),\ \omega\geq 0;\ =0, elsewhere)$ is the *j*-th (stationary) one-sided power spectral density of process $f_j^C(t)$, $(j=1,2,...,m)$. Note that eq. (23) actually provides the 50% fractile of distribution of maxima that can be assumed coincident with the mean value of the peak values [49]. Equation (23) provides the vehicle for determining the power spectral density of the corrective vector process $G_j^C(\omega)$. Specifically, taking into account eqs. (22) and (23) and imposing the equivalency between the ensemble-averaged response spectra $RSA^{(f_j^{SC})}(\omega)$ and the target response spectra $RSA^{(j)}(\omega)$ $(j=1,...,m)$, it is straightforward to show after some simple algebra that the following relation holds:

$$(RSA^{(j)}(\omega_0))^2 - (RSA^{(f_L^j)}(\omega_0))^2 = \omega_0^4 \left(\eta_{U^C}^{(j)}\right)^2 \lambda_{0,U^C}^{(j)} \qquad \forall\, RSA^{(j)}(\omega_0) > RSA^{(f_L^j)}(\omega_0) \tag{25}$$

The power spectral density of the *j*-th component of the corrective process $f_j^C(t)$, $(j=1,2,...,m)$ can be determined using the recursive procedure proposed in [45]:

$$G_j^C(\omega) = 0 \qquad 0\leq\omega\leq\omega_{lc}\ , \tag{26}$$

$$G_j^C(\omega_i) = \frac{4\zeta_0}{\omega_i\pi - 4\zeta_0\omega_{i-1}}\left(\frac{\left(RSA^{(j)}(\omega_i,\zeta_0)\right)^2 - \left(RSA^{(f_j^L)}(\omega_i,\zeta_0)\right)^2}{\left(\eta_{U^C}^{(j)}(\omega_i,\zeta_0)\right)^2} - \Delta\omega\sum_{r=1}^{i-1} G_j^C(\omega_r)\right), \qquad \omega_{lc}<\omega\leq\omega_c$$

(27)

where $\omega_i = \omega_{lc} + i\,\Delta\omega$ and η_{U^C} is set equal to:

$$\eta_{U^C}^{(j)}(\omega_i, \zeta_0, T_s, p = 0.5) = \sqrt{2\ln\left\{2N_{U^C}^{(j)}\left[1 - exp\left[-\left(\delta_{U^C}^{(j)}\right)^{1.2}\sqrt{\pi\ln\left(2N_{U^C}^{(j)}\right)}\right]\right]\right\}} \tag{28}$$

with:

$$N_{U^C}^{(j)} = \frac{T_s}{2\pi}\omega_i\left(-\ln p\right)^{-1} \tag{29}$$

$$\delta_{U^C}^{(j)} = \left[1 - \frac{1}{1-\zeta_0^2}\left(1 - \frac{2}{\pi}\arctan\frac{\zeta_0}{\sqrt{1-\zeta_0^2}}\right)^2\right]^{1/2} \tag{30}$$

approximately determined according to the hypothesis of a barrier outcrossing in clumps and spectral moments determined assuming that the input power spectral density has a smooth shape and $\zeta_0 << 1$. Moreover, $\omega_{lc} \cong 1$ rad/s is the lowest bound in the domain of η_{U^C} while ω_c represents an upper cut-off frequency beyond which the elements of $G_j^C(\omega_i)$ may be assumed to be zero. The accuracy of the power spectral density of each individual corrective term can be iteratively improved via the equation:

$$G_j^C(\omega)\Big|_k = G_j^C(\omega)\Big|_{k-1}\left[\frac{\left(RSA^{(j)}(\omega,\zeta_0)\right)^2}{\left(RSA^{(f_L^j)}(\omega,\zeta_0)\right)^2 + \left(RSA^{(f_C^j)}(\omega,\zeta_0)\right)^2\Big|_{k-1}}\right], \tag{31}$$

where $\left(RSA^{(f_C^j)}(\omega,\zeta_0)\right)\Big|_k$ represents the response spectrum of the corrective term determined at the k-th iteration. It should be noted that the iterations stop as soon as equation (19) is satisfied.

After determining the power spectral density function of each corrective term, the elements of the evolutionary spectrum-compatible cross-spectral density matrix $\mathbf{S}_f^{SC}(\omega,t)$ are established as follows:

$$\begin{aligned} S_{jj}^{SC}(\omega,t) &= S_{jj}^{L}(\omega,t) + S_{j}^{C}(\omega,t), && j=1,2,...,m \\ S_{jk}^{SC}(\omega,t) &= \sqrt{S_{jj}^{SC}(\omega,t)S_{kk}^{SC}(\omega,t)}\,\Gamma_{jk}(\omega), && j,k=1,2,...,m; \quad j\neq k \end{aligned} \tag{32}$$

Finally, fully non-stationary ground motion time histories that reflect a prescribed coherence function $\Gamma_{jk}(\omega)$ and are compatible with prescribed response spectra can be generated using the procedure proposed by Deodatis [38] (described in previous sections), using for the evolutionary cross-spectral density matrix $\mathbf{S}_f^0(\omega,t)$, the computed spectrum-compatible one: $\mathbf{S}_f^{SC}(\omega,t)$. The proposed methodology is also summarized in flow-chart form in Figure 1.

The methodology proposed in this paper (outlined in Fig. 1) to simulate fully non-stationary ground motion time histories at a number of locations on the ground surface that reflect a prescribed coherence function and are compatible with prescribed response spectra does not require any iterations on the individual generated sample functions. This is probably the most important advantage/innovation of the proposed methodology as Gaussianity and coherence structure of every generated sample vector process are guaranteed. It is known that if iterations are involved with the generation of sample functions, Gaussianity and coherence structure deteriorate (e.g. Deodatis and Micaletti [50]), unless the iterations are random in nature (e.g. Bocchini and Deodatis [51]). However, in the latter case, the computational cost increases drastically.

5 NUMERICAL EXAMPLES

In this section, the proposed methodology for generating fully non-stationary and spectrum-compatible ground motion vector processes is demonstrated with a numerical example. For this purpose, consider the configuration of points depicted in Figure 2, representing three different

locations where fully non-stationary ground motion time histories compatible with three different response spectra defined by Eurocode 8 [47] have to be simulated. Specifically, point 1 corresponds to type A soil (rock or other rock-like geological formation), point 2 corresponds to type B soil (deposits of very dense sand, gravel, or very stiff clay), while point 3 corresponds to type D soil (deposits of loose-to-medium cohesionless soil or of predominantly soft-to-firm cohesive soil).

Furthermore, the maximum ground acceleration a_g has been set equal to $0.35g$ for each location. According to the proposed methodology, the 1D-3V (one dimensional, tri-variate), non-stationary, zero-mean, Gaussian stochastic vector process $\boldsymbol{f}^L(t)$ having evolutionary cross-spectral density matrix:

$$\boldsymbol{S}^L(\omega,t)=\begin{pmatrix} S_{11}^L(\omega,t) & S_{12}^L(\omega,t) & S_{13}^L(\omega,t) \\ S_{21}^L(\omega,t) & S_{22}^L(\omega,t) & S_{23}^L(\omega,t) \\ S_{31}^L(\omega,t) & S_{32}^L(\omega,t) & S_{33}^L(\omega,t) \end{pmatrix} \tag{33}$$

has to be defined first. The Clough-Penzien acceleration spectrum is selected to model the non-separable power spectral density functions $S_{jj}^L(\omega,t);\ j=1,2,3$ (all three spectra are assumed to be identical to each other here):

$$S_{jj}^L(\omega,t)=A(t)^2 S_0(t)\frac{\left(1+4\zeta_g^2(t)\left(\frac{\omega}{\omega_g(t)}\right)^2\right)}{\left(1-\left(\frac{\omega}{\omega_g(t)}\right)^2\right)^2+4\zeta_g^2(t)\left(\frac{\omega}{\omega_g(t)}\right)^2}\frac{\left(\frac{\omega}{\omega_f(t)}\right)^4}{\left(1-\left(\frac{\omega}{\omega_f(t)}\right)^2\right)^2+4\zeta_f^2(t)\left(\frac{\omega}{\omega_f(t)}\right)^2} \tag{34}$$

The off-diagonal terms are defined as:

$$S_{jk}^L(\omega,t)=S_{jj}^L(\omega,t)\Gamma_{jk}(\omega)=S_{kk}^L(\omega,t)\Gamma_{jk}(\omega) \tag{35}$$

where $\Gamma_{jk}(\omega)=\gamma_{jk}(\omega)\exp\left[-i\omega\xi_{jk}/v\right]$, $\gamma_{jk}(\omega)$ is the coherence function, and $\exp\left[-i\omega\xi_{jk}/v\right]$ is the wave propagation term with ξ_{jk} being the distance between points *j* and *k*, and *v* being the

apparent velocity of wave propagation. The Harichandran-Vanmarcke [52] model is chosen to model the coherence function:

$$\gamma_{jk}(\omega) = a\exp\left[-\frac{2\xi_{jk}}{\alpha\theta(\omega)}(1-a+\alpha a)\right] + (1-a)\exp\left[-\frac{2\xi_{jk}}{\theta(\omega)}(1-a+\alpha a)\right] \tag{36}$$

The above models for the evolutionary spectra and coherence function have been selected for illustrative purpose only. Alternatively, different models can be used in a straightforward manner. Pertinent parameters used in this numerical example include:

$$\omega_g(t) = 20 - 7\frac{t}{30};\ \zeta_g(t) = 0.6 - 0.2\frac{t}{30};\ \omega_f(t) = 0.1\omega_g(t);\ \zeta_f(t) = \zeta_g(t) \tag{37}$$

and:

$$A(t) = a_1 t\exp\left(-a_2 t\right);\quad a_1 = 0.68\,s^{-1};\ a_2 = 1/4\,s^{-1}; \tag{38}$$

Furthermore:

$$S_0(t) = \frac{\sigma^2}{\pi\omega_g(t)\left(2\zeta_g(t) + \dfrac{1}{2\zeta_g(t)}\right)};\quad \sigma = 100\,cm/s^2 \tag{39}$$

In Figures 3 and 4 the evolutionary spectra $S_{11}(\omega,t) = S_{22}(\omega,t) = S_{33}(\omega,t)$ and the coherence functions $\gamma_{jk}(\omega)$ $(j,k = 1,2,3;\ j \neq k)$ are displayed assuming [38]:

$$a = 0.626;\quad \alpha = 0.022;\quad k = 19,700\,m;\ \ \Omega = 12.692\,rad/s,\quad b = 3.47 \tag{40}$$

and:

$$\theta(\omega) = k\left[1 + \left(\frac{\omega}{\Omega}\right)^b\right]^{-1/2}. \tag{41}$$

Figure 5a compares the target response spectra $RSA^{(j)}(T)$ $(j = 1,2,3)$ to the ensemble averaged simulated response spectra $RSA^{(f_j^L)}(T)$, as a function of the natural period. In order to minimize the

influence of the corrective term $f_j^C(t)$ on the non-stationary characteristics of the corresponding term $f_j^L(t)$, each of the $f_j^L(t)$ terms $(j=1,2,3)$ is scaled so its response spectrum $RSA^{(f_j^L)}(\omega)$ matches the corresponding target response spectrum $RSA^{(j)}(\omega)$ at at least one point and at the same time $RSA^{(f_j^L)}(\omega) \le RSA^{(j)}(\omega)$ at every frequency. Figure 5b displays the scaled $RSA^{(f_1^L)}(T)$ together with $RSA^{(1)}(T)$, Figure 5c the scaled $RSA^{(f_2^L)}(T)$ together with $RSA^{(2)}(T)$, and Figure 5d the scaled $RSA^{(f_3^L)}(T)$ together with $RSA^{(3)}(T)$. As indicated in Figures 5b - 5d, the matching can occur at different periods, depending on the shapes of the evolutionary power spectral densities of the local components $f_j^L(t)$.

The (stationary) power spectral density functions of the corrective process $f_j^C(t)$ $(j=1,2,3)$ are determined using eqs. (26) and (27). The Jennings, Housner and Tsai model [53] is selected for the modulating function of the corrective term (refer to eq. (21)):

$$\varphi(t) = \begin{cases} \left(\dfrac{t}{t_1}\right)^2 & t < t_1 \\ 1 & t_1 \le t \le t_2 \\ \exp\left[-\beta\left(t-t_2\right)\right] & t > t_2 \end{cases} \tag{42}$$

whose parameters t_1 and t_2 are determined so as to preserve the strong motion segment of the process $\boldsymbol{f}^L(t)$ via the so-called Husid function (see e.g. [45]) herein extended to stochastic processes:

$$E_L^{(j)}(t) = \frac{\int_0^t \int_0^\infty S_{jj}^L(\omega,t)\,d\omega\,dt}{\int_0^{t_f} \int_0^\infty S_{jj}^L(\omega,t)\,d\omega\,dt}; \qquad 0 \le E_L^{(j)}(t) \le 1; \quad (j=1,2,3) \tag{43}$$

with t_f being the duration of the process. Following eq. (43), $t_1 = 1.65\,s$ and $t_2 = 12.7\,s$ are the time instants for which function $E_L^{(1)}(t) = E_L^{(2)}(t) = E_L^{(3)}(t)$ assumes the values of 0.05 and 0.95 respectively. Parameter β is set equal to $0.1734\,s^{-1}$. It follows that $T_S = t_2 - t_1 = 11.05\,s$ satisfies the limit imposed by the code ($T_S \geq 10\,s$) [47].

The evolutionary and spectrum-compatible cross-spectral density matrix is then evaluated using equation (32). Its diagonal elements, along with the scaled $S_{jj}^L(\omega,t)$ and $S_j^C(\omega,t)$; $j = 1,2,3$, are plotted in Figure 6. Then, fully non-stationary spectrum-compatible earthquakes are generated using eq. (16). A typical sample for each component is provided in Figure 7. A comparison of the ensemble-averaged simulated response spectra (using 100 samples) with the target ones confirms the effectiveness of the proposed methodology (Figure 8). Figure 9 compares the ensemble-averaged coherence functions obtained from 10,000 simulated sample functions with the prescribed ones defined in equation (36), indicating an excellent agreement (the estimation of the coherence function from sample time histories is notoriously difficult (e.g. Zerva 2009) and consequently a much larger number of sample functions is used when compared to the estimation of the response spectra). Finally, Figure 10 plots on normal probability paper the empirical probability distribution functions of generated sample functions at time instant $t = 5s$ using 10,000 samples. The agreement with the Gaussian distribution is excellent (10,000 samples are considered roughly necessary to estimate the probability distribution reasonably well).

6 CONCLUDING REMARKS

In this paper, a spectral-representation-based methodology has been proposed for generating sample functions of fully non-stationary and spectrum-compatible ground motion time histories at a number of locations on the ground surface that reflect prescribed coherence functions. The basic idea of the methodology considers that the stochastic vector process modelling ground motion is constructed

by the superposition of two components: the first is an evolutionary non-stationary stochastic vector process with amplitude and frequency modulation, representative of local geological and seismological conditions. The second one is a corrective term modelled by a quasi-stationary stochastic vector process (a non stationary process with only amplitude modulation) that adjusts the response spectra of the overall vector process to make them response spectrum-compatible. The proposed methodology is not requiring any iteration on the individual generated sample functions, thus preserving the Gaussianity and coherence structure of every generated sample vector process. The methodology has also the advantage of providing the fully non-stationary and spectrum-compatible cross spectral density matrix of the ground motion time histories that can be used for reliability studies in an analytic stochastic fashion.

REFERENCES

[1] Hao, H. and Duan, X. N. (1995). Seismic response of asymmetric structures to multiple ground motions. *Journal of Structural Engineering*, ASCE, 121(11), 1557–1564.

[2] Hao, H. (1997). Torsional response of building structures to spatial random ground excitations. *Engineering Structures*, 19(2), 105–112.

[3] Herdia-Zavoni, E. and Barranco, F. (1996). Torsion in symmetric structures due to ground-motion spatial variation. *Journal of Engineering Mechanics*, ASCE, 122(9), 834–843.

[4] Hahn, G. D. and Liu, X. (1994). Torsional response of unsymmetric buildings to incoherent ground motions. *Journal of Structural Engineering*, ASCE, 120(4), 1158–1181.

[5] Zerva, A. (1990). Response of multi-span beams to spatially incoherent seismic ground motions, Earthquake Engineering and Structural Dynamics, 19, 819-832.

[6] Zerva, A. (1991). Effect of spatial variability and propagation of seismic ground motions on the response of multiply supported structures. *Probabilistic Engineering Mechanics*, 7, 217–226.

[7] Abrahamson, N. A. (1993). Spatial variation of multiple support inputs. Proceedings, 1st U. S. Seminar on Seismic Evaluation and Retrofit of Steel Bridges, Department of Civil Engineering and California Department of Trans-portation, University of California at Berkeley, San Francisco, California.

[8] Harichandran, R. S., Hawwari, A. and Sweidan, B. (1996). Response of long-span bridges to spatially varying ground motion. *Journal of Structural Engineering*, ASCE, 122(5), 476–484.

[9] Hao, H. (1993). Arch responses to correlated multiple excitations. *Earthquake Engineering and Structural Dynamics*, 22(5), 389–404.

[10] Hao, H. (1994). Ground-motion spatial variation effects on circular arch responses. *Journal of Engineering Mechanics*, ASCE, 120(11), 2326.

[11] Chen MT and Harichandran, R. S, (2001) Response of an earth dam to spatially varying earthquake ground motion, *Journal of Engineering Mechanics*, 127(9), 932-939

[12] Luco, J. E. and Mita, A. (1987). Response of circular foundation to spatially varying random ground motion. *Journal of Engineering Mechanics*, ASCE, 113(1), 1–15.

[13] Luco, J. E. and Wong, H. L. (1986). Response of a rigid foundation to a spatially random ground motion. *Earthquake Engineering and Structural Dynamics*, 14, 891–908.

[14] Soliman H. O. Datta T. K. , (1996) Response of overground pipelines to random ground motion *Engineering Structures*, 18,(7), 537-545.

[15] Zerva A. (1993). Pipeline response to directionally and spatially correlated seismic ground motions, *Journal of Pressure Vessel Technology*, ASME, 115, 53-58

[16] Ghobarah, A., Aziz, T. S. and El-Attar, M. (1996). Response of transmission lines to multiple support excitation. *Engineering Structures*, 18(12), 936–946.

[17] Abrahamson, N. A. (2007), Hard-rock coherency functions based on the Pinyon Flat array data" Draft report to EPRI, Electric Power Research Institute, Palo Alto, CA.

[18] Zerva A. (2009), *Spatial variation of seismic ground motions: modelling and engineering applications*, CRC Press, Taylor & Francis Group.

[19] Berrah, M. K. and Kausel, E. (1993). A modal combination rule for spatially varying seismic motions. *Earthquake Engineering and Structural Dynamics*, 22(9), 791–800.

[20] Zembaty, Z. and Krenk, S. (1994). Spatial seismic excitations and response spectra. *Journal of Engineering Mechanics*, ASCE, 119(12), 2449–2460.

[21] Allam SM. and Datta TK (2002) Response Spectrum Analysis of Suspension Bridges for Random Ground Motion, *Journal of Bridge Engineering*, 7(6), 325-337.

[22] Der Kiureghian, A. and Neuenhofer, A. (1992). Response spectrum method for multi-support seismic excitations. *Earthquake Engineering and Structural Dynamics*, 21(8), 713–740.

[23] Heredia-Zavoni, E. and Vanmarcke, E. H. (1994). Seismic random-vibration analysis of multisupport-structural systems. *Journal of Engineering Mechanics*, ASCE, 120(5), 1107–.1127

[24] Shinozuka M. (1971), Simulation of multivariate and multidimensional random processes. *Journal of Acoustic Society of America*;49:357–67.

[25] Mignolet M. P. & Spanos P.-T. D. (1987), Recursive simulation of stationary multi-variate random processes. Part I. *J. Appl. Mech*., 54 674-80.

[26] Mignolet M. P. & Spanos, P.-T. D., (1987) Recursive simulation of stationary multi-variate random processes. Part II. *J. Appl. Mech*., 54 681-7.

[27] Shinozuka, M. and Deodatis, G. (1988), Stochastic process models of earthquake ground motion. *Journal of Probabilistic Engineering Mechanics*, 3(3) 114-123.

[28] Zerva, A. (1992) Seismic ground motion simulations from a class of spatial variability models, *Earthquake Engineering and Structural Dynamics*, 7, 217-226

[29] Ramadan O. and Novak M. (1993). Simulation of spatially incoherent random ground motion. *Journal of Eng-neering Mechanics*, ASCE, 119(5), 997–1016.

[30] Vanmarcke E., Heredia-Zavoni E. and Fenton, G. A. (1993). Conditional simulation of spatially correlated earthquake ground motion. *Journal of Engineering Mechanics*, ASCE, 119(11), 2333–2352.

[31] Ramadan O. and Novak M. (1994). Simulation of multidimensional, anisotropic ground motions. *Journal of Engineering Mechanics*, ASCE, 120(8), 1773–1785.

[32] Li Y. and Kareem A. (1993), Simulation of multi-variate random processes: hybrid DFT and digital filtering approach. *J. Engng Mech*., ASCE, 119 1078-98.

[33] Deodatis G. (1996), Simulation of ergodic multi-variate stochastic processes. *J. Engng Mech*., ASCE, 122, 778-787.

[34] Di Paola M. and Zingales M (2003). Stochastic seismic analysis of hydrodynamic pressure in dam reservoir systems *Earthquake Engineering & Structural Dynamics* 32 (1): 165-172.

[35] Shama AA. (2007), Simplified procedure for simulating spatially correlated earthquake ground motions, *Engineering Structures*, 2,9 248–258.

[36] Zentner, I., (2007) Simulation of spatially incoherent, non stationary seismic free field motion and its impact on response in SSI analysis, ECCOMAS Thematic Conference on Computational Methods in Structural Dynamics and Earthquake Engineering, 13-16 June 2007.

[37] Zerva A and Shinozuka M. (1991), Stochastic differential ground motion, *Structural Safety*, 10, 129-143.

[38] Deodatis G (1996), Non-stationary stochastic vector processes: seismic ground motion applications", *Probabilistic Engineering Mechanics*, 11, 149-168

[39] Hao H., Oliveira C. S. and Penzien J. (1989), Multiple-station ground motion processing and simulation based on SMART-1 array data. *Nuclear Engng and Design*, 111, 293-310.

[40] Yeh C.H. and Wen Y.K. (1990) Modeling of non-stationary ground motion and analysis of inelastic structural response. *Structural Safety* ; 8(1-4): 281-298.

[41] Wang J, Fan L, Qian S. and Zhou J (2002) Simulations of non-stationary frequency content and its importance to seismic assessment of structures, *Earthquake Engineering and Structural Dynamics*; 31: 993-1005.

[42] Spanos PD, Giaralis A, Politis NP (2007), Time-frequency representation of earthquake accelerograms and inelastic structural response records using the adaptive chirplet decomposition and empirical mode decomposition. *Soil Dynamics and Earthquake Engineering* 27 (7): 675-689.

[43] Priestley, M.B.: (1981) *Spectral Analysis and Time Series*. Academic Press.

[44] Sarkar, K. and V.K. Gupta (2005). Wavelet-based simulation of Spatially Correlated and Spectrum-Compatible Accelerograms, Proc. National Symposium on Structural Dynamics, Random Vibrations & Earthquake Engineering (NSSD-2005), Department of Civil Engineering, Indian Institute of Science, Bangalore, 69-78.

[45] Cacciola, P. (2010). A stochastic approach for generating spectrum compatible fully nonstationary earthquakes , *Computers and Structures*, 88 (15-16). pp. 889-901.

[46] International Conference of Building Officials, Uniform Building Code, Vol. 2, 1997

[47] European Committee For Standardization (2003), Eurocode 8: Design of structures for earthquake resistance -Part 1: General rules, seismic actions and rules for buildings¸ Brussels, Belgium.

[48] Rosenblueth, E. (1951). A basis for aseismic design. PhD thesis, Univ. of Illinois, Urbana, Ill.

[49] Vanmarcke EH, Gasparini DA. (1977) Simulated earthquake ground motions. Proc. 4th Int. Conf. on Smirt, K1/9, San Francisco1977.

[50] Deodatis G. and Micaletti R.C., (2001) Simulation of highly skewed non-Gaussian stochastic processes, *Journal of Engineering Mechanics* (ASCE) 127 (12), 1284–1295.

[51] Bocchini P. and Deodatis G., (2008), Critical review and latest developments of a class of simulation algorithms for strongly non-Gaussian random fields, *Probabilistic Engineering Mechanics* 23, 393–407.

[52] Harichandran, RS and Vanmarke EH, (1986), Stochastic variation of earthquake ground motion in space and time, *J. Engng Mech*, ASCE, 112, 154-74.

[53] Jennings, P.C., Housner, G.W., Tsai C. (1969) Simulated earthquake motions for design purpose. Proc. 4th World Conference Earth. Eng. Santiago, vol. A-1: 145-160.

FIGURE CAPTIONS

Figure 1: Flow chart of the proposed methodology for generating fully non-stationary and spectrum-compatible ground motion vector processes

Figure 2: Configuration of points 1, 2 and 3 on the ground surface depicted along with their corresponding target response spectra

Figure 3: Evolutionary power spectral density functions $S_{jj}^{L}(\omega,t),\ (j=1,2,3)$

Figure 4: Prescribed coherence functions $\gamma_{jk}(\omega)\ \ (j,k=1,2,3;\ \ j\neq k)$

Figure 5: a) Comparison between the ensemble-averaged simulated response spectra $RSA^{(f_1^L)}(T)=RSA^{(f_2^L)}(T)=RSA^{(f_3^L)}(T)$ before scaling with the target ones $RSA^{(j)}(T)$ $(j=1,2,3)$, b) Comparison between the scaled $RSA^{(f_1^L)}(T)$ and $RSA^{(1)}(T)$ $(\alpha_1=0.71)$, c) Comparison between the scaled $RSA^{(f_2^L)}(T)$ and $RSA^{(2)}(T)$ $(\alpha_2=1.08)$, d) Comparison between the scaled $RSA^{(f_3^L)}(T)$ and $RSA^{(3)}(T)$ $(\alpha_3=1.55)$.

Figure 6: a) Evolutionary power spectral density functions $S_{jj}^{L}(\omega,t),\ (j=1,2,3)$ after scaling with $\alpha_1=0.71;\ \alpha_2=1.08;\ \alpha_3=1.55$; b) Evolutionary power spectral density functions of the corrective quasi-stationary process $S_j^C(\omega,t),\ (j=1,2,3)$; c) Evolutionary spectrum-compatible power spectral density functions $S_{jj}^{SC}(\omega,t),\ (j=1,2,3)$

Figure 7: Generated spectrum-compatible sample function for the acceleration at points 1,2 and 3

Figure 8: Comparison between the ensemble-averaged simulated response spectra $RSA^{(f_j^{SC})}(T)$ and the corresponding target ones $RSA^{(j)}(T)$ $(j=1,2,3)$ using 100 samples.

Figure 9: Comparison between the prescribed and ensemble-averaged simulated coherence functions $\gamma_{jk}(\omega)\ \ (j,k=1,2,3;\ \ \ j\neq k)$ using 10,000 samples.

Figure 10: Empirical probability distribution functions of generated sample functions at time instant $t=5s$ using 10,000 samples (plots on normal probability paper).

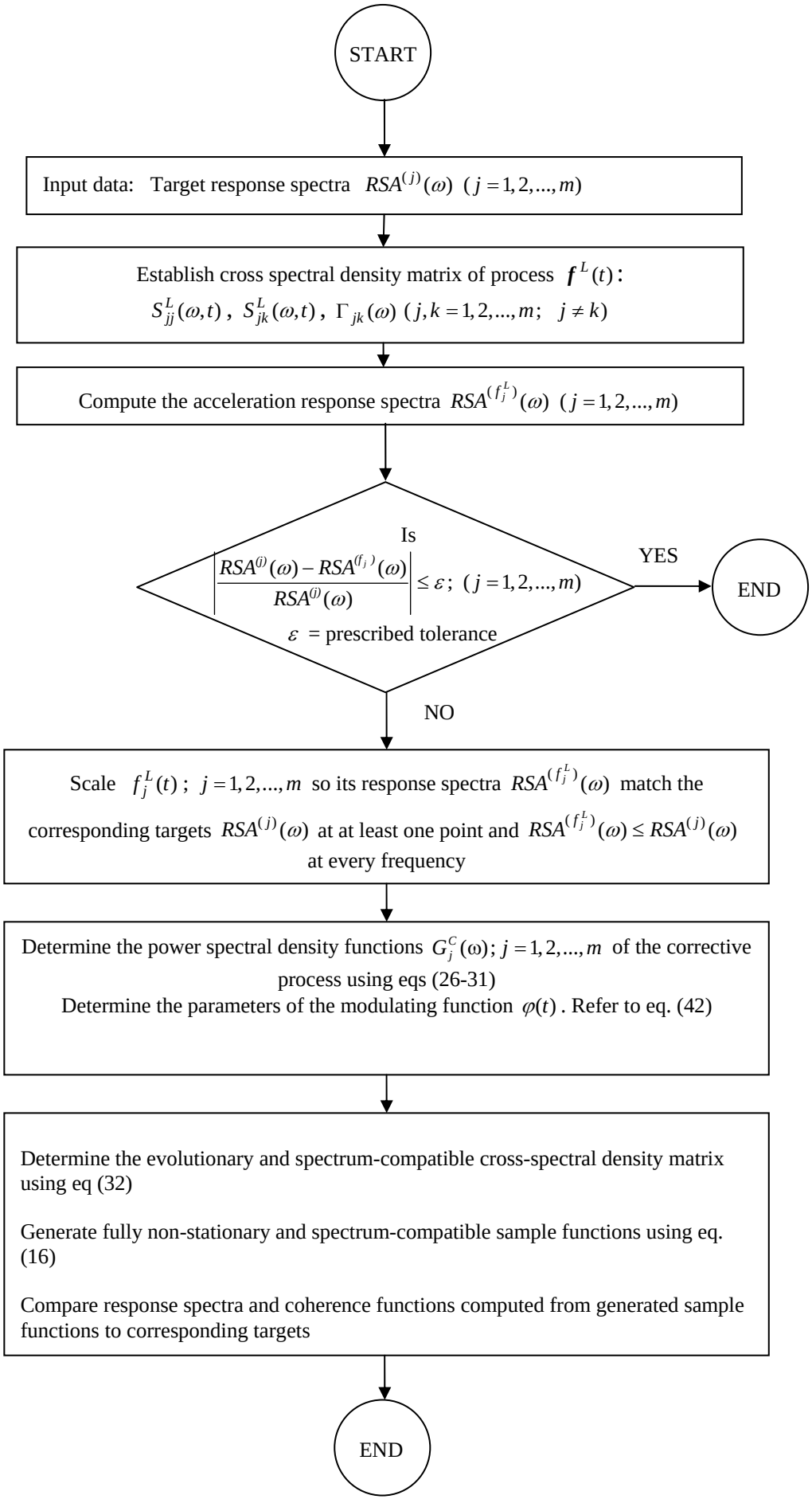
START
Input data: Target response spectra $RSA^{(j)}(\omega)$ $(j=1,2,...,m)$
Establish cross spectral density matrix of process $\boldsymbol{f}^L(t)$:
$S_{jj}^L(\omega,t)$, $S_{jk}^L(\omega,t)$, $\Gamma_{jk}(\omega)$ $(j,k=1,2,...,m;\ j\neq k)$
Compute the acceleration response spectra $RSA^{(f_j^L)}(\omega)$ $(j=1,2,...,m)$
Is
$\left|\frac{RSA^{(j)}(\omega)-RSA^{(f_j)}(\omega)}{RSA^{(j)}(\omega)}\right|\leq\varepsilon;\ (j=1,2,...,m)$
ε = prescribed tolerance
YES
END
NO
Scale $f_j^L(t)$; $j=1,2,...,m$ so its response spectra $RSA^{(f_j^L)}(\omega)$ match the corresponding targets $RSA^{(j)}(\omega)$ at at least one point and $RSA^{(f_j^L)}(\omega)\leq RSA^{(j)}(\omega)$ at every frequency
Determine the power spectral density functions $G_j^C(\omega);\ j=1,2,...,m$ of the corrective process using eqs (26-31)
Determine the parameters of the modulating function $\varphi(t)$. Refer to eq. (42)
Determine the evolutionary and spectrum-compatible cross-spectral density matrix using eq (32)
Generate fully non-stationary and spectrum-compatible sample functions using eq. (16)
Compare response spectra and coherence functions computed from generated sample functions to corresponding targets
END

Figure 1

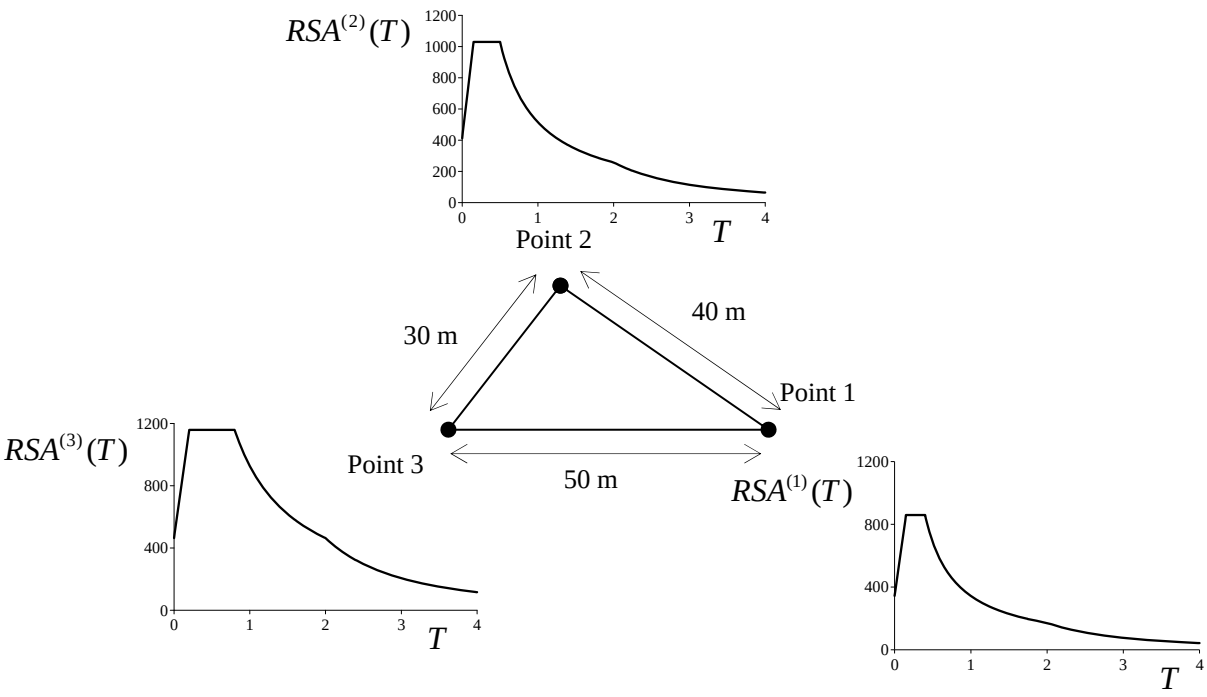
$RSA^{(2)}(T)$
1200
1000
800
600
400
200
0
0
1
2
3
4
T
Point 2
30 m
40 m
Point 1
Point 3
50 m
$RSA^{(3)}(T)$
1200
800
400
0
0
1
2
3
4
T
$RSA^{(1)}(T)$
1200
800
400
0
0
1
2
3
4
T

Figure 2

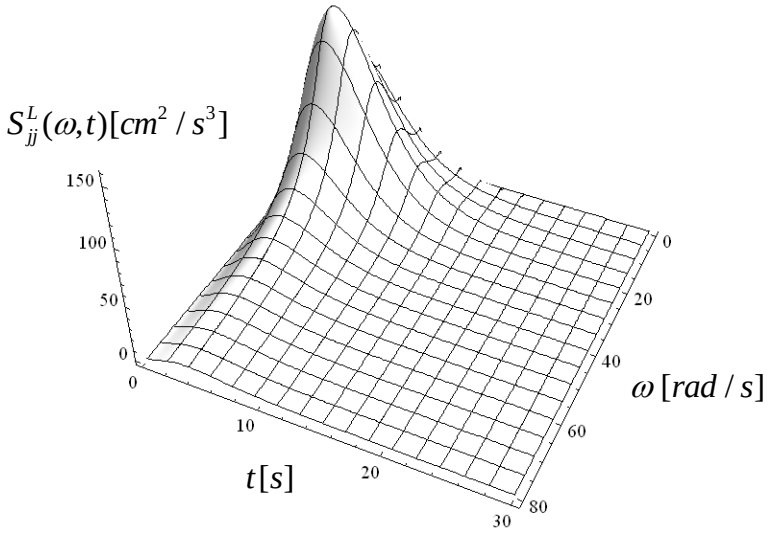
$S_{jj}^{L}(\omega,t)[cm^2/s^3]$
150
100
50
0
0
10
20
30
$t[s]$
0
20
40
60
80
$\omega\,[rad/s]$

Figure 3

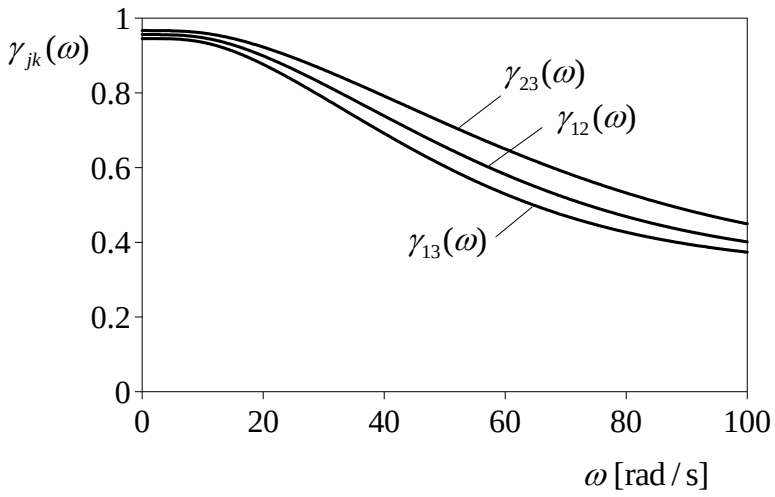
$\gamma_{jk}(\omega)$
1
0.8
0.6
0.4
0.2
0
0
20
40
60
80
100
ω [rad / s]
$\gamma_{23}(\omega)$
$\gamma_{12}(\omega)$
$\gamma_{13}(\omega)$

Figure 4

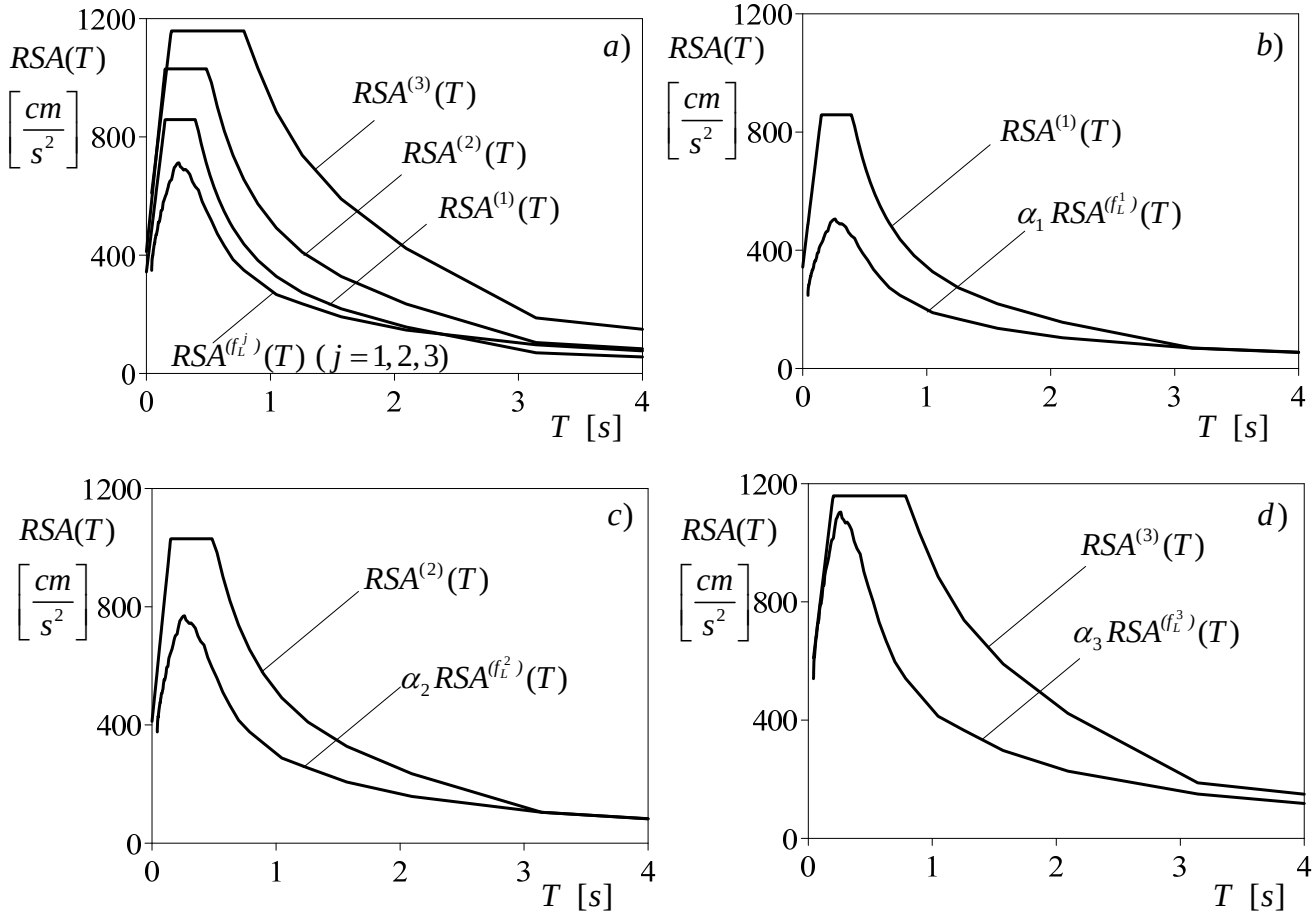
a)
b)
c)
d)
RSA(T)
cm/s²
T [s]
RSA^(3)(T)
RSA^(2)(T)
RSA^(1)(T)
RSA^(f_L^j)(T) (j = 1,2,3)
α1 RSA^(f_L^1)(T)
α2 RSA^(f_L^2)(T)
α3 RSA^(f_L^3)(T)
0
400
800
1200
1
2
3
4

Figure 5

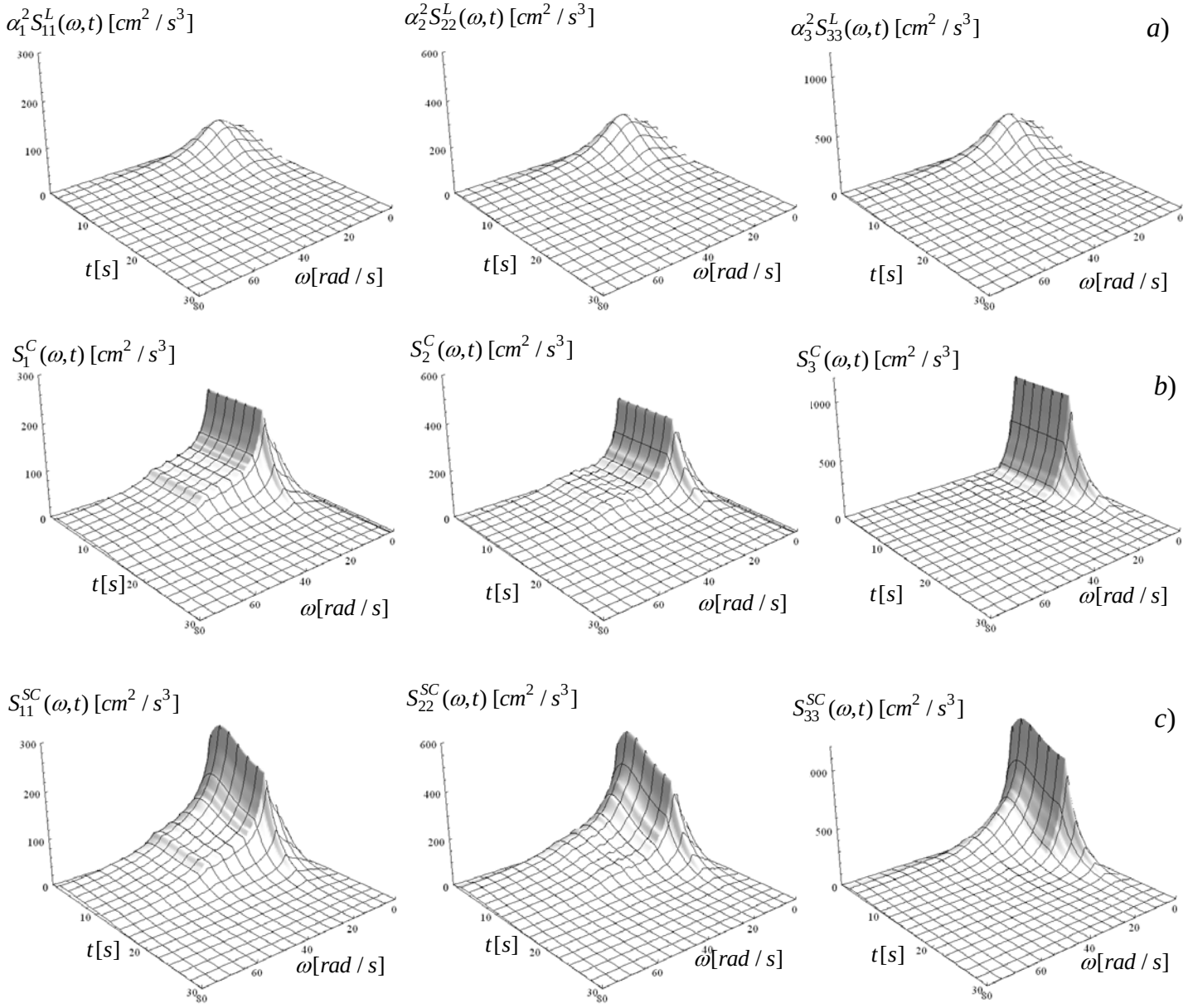
$\alpha_1^2 S_{11}^L(\omega,t)\ [cm^2/s^3]$
$\alpha_2^2 S_{22}^L(\omega,t)\ [cm^2/s^3]$
$\alpha_3^2 S_{33}^L(\omega,t)\ [cm^2/s^3]$
a)
$S_1^C(\omega,t)\ [cm^2/s^3]$
$S_2^C(\omega,t)\ [cm^2/s^3]$
$S_3^C(\omega,t)\ [cm^2/s^3]$
b)
$S_{11}^{SC}(\omega,t)\ [cm^2/s^3]$
$S_{22}^{SC}(\omega,t)\ [cm^2/s^3]$
$S_{33}^{SC}(\omega,t)\ [cm^2/s^3]$
c)
t[s]
ω[rad / s]

Figure 6

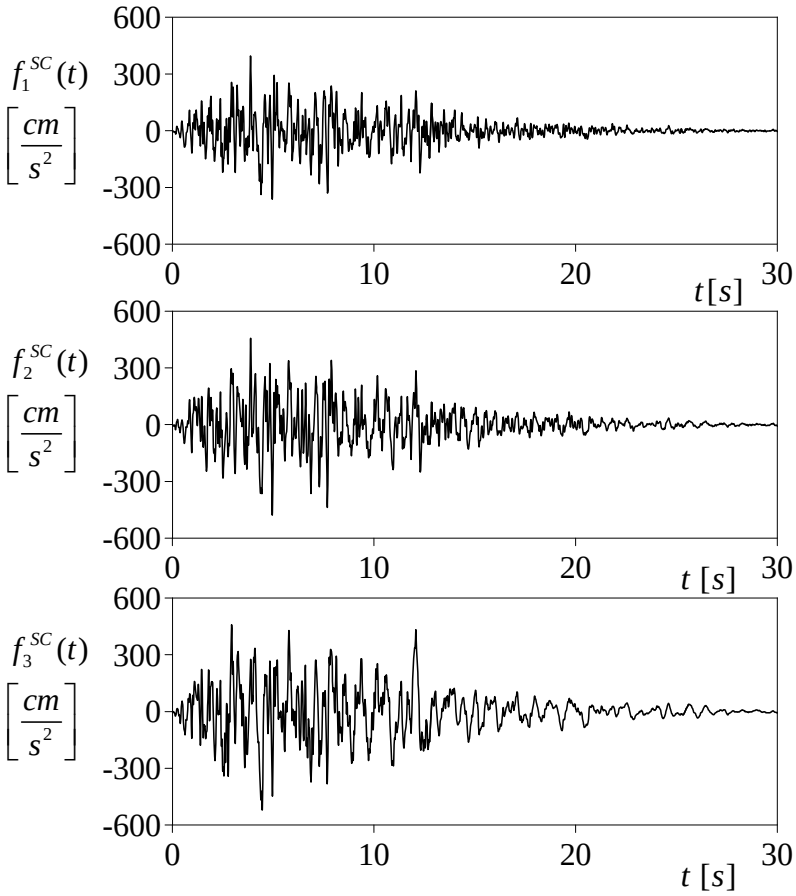
$f_1^{SC}(t)$
$\left[\frac{cm}{s^2}\right]$
600
300
0
-300
-600
0
10
20
30
$t[s]$
$f_2^{SC}(t)$
$\left[\frac{cm}{s^2}\right]$
600
300
0
-300
-600
0
10
20
30
$t\ [s]$
$f_3^{SC}(t)$
$\left[\frac{cm}{s^2}\right]$
600
300
0
-300
-600
0
10
20
30
$t\ [s]$

Figure 7

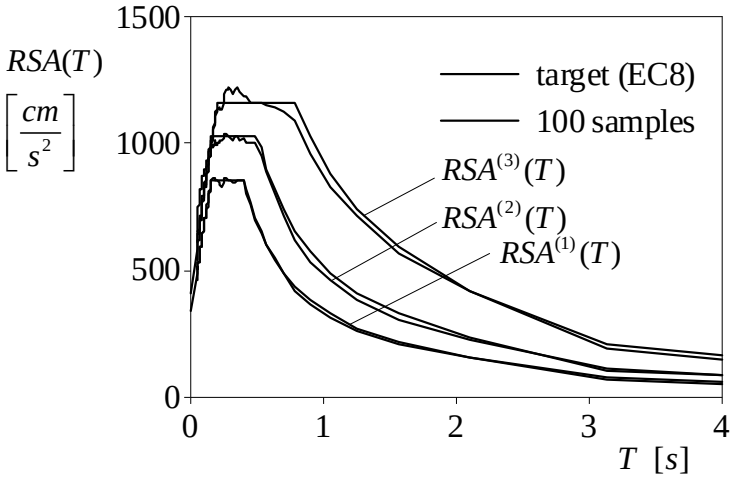
RSA(T)
[cm/s²]
1500
1000
500
0
0
1
2
3
4
T [s]
target (EC8)
100 samples
RSA(3)(T)
RSA(2)(T)
RSA(1)(T)

Figure 8

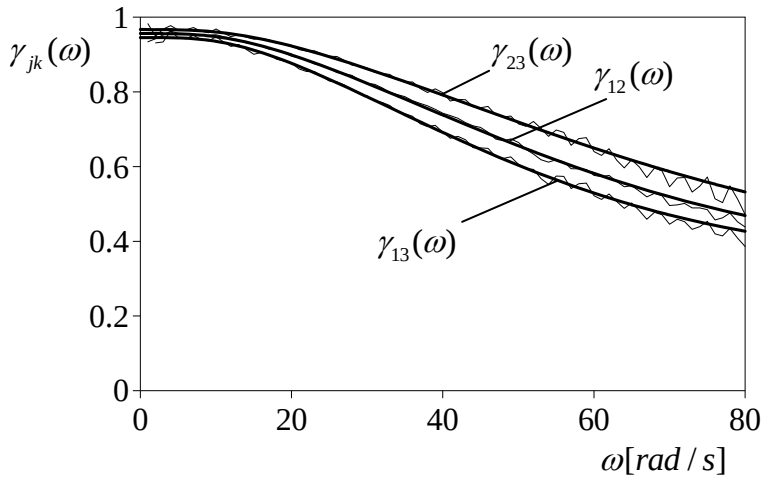
$\gamma_{jk}(\omega)$
1
0.8
0.6
0.4
0.2
0
0
20
40
60
80
$\omega[rad/s]$
$\gamma_{23}(\omega)$
$\gamma_{12}(\omega)$
$\gamma_{13}(\omega)$

Figure 9

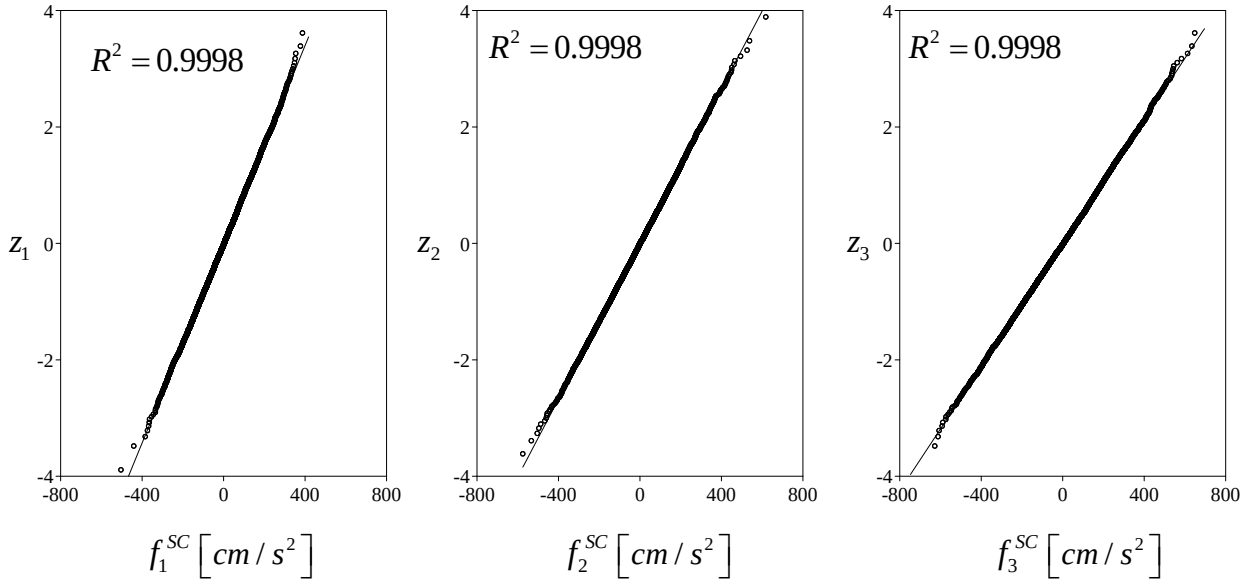
$R^2 = 0.9998$
z_1
$f_1^{SC}\left[cm/s^2\right]$
$R^2 = 0.9998$
z_2
$f_2^{SC}\left[cm/s^2\right]$
$R^2 = 0.9998$
z_3
$f_3^{SC}\left[cm/s^2\right]$

Figure 10